COBEM 99
XV Congresso Brasileiro de Engenharia Mecânica
15th Brazilian Congress of Mechanical Engineering
22 - 26 de Novembro de 1999 / November 22 - 26, 1999 Águas de Lindóia, São Paulo,

AN ORDER OF ACCURACY ANALYSIS FOR FLUX-VECTOR SPLITTING SCHEMES ON UNSTRUCTURED GRIDS

João Luiz F. Azevedo
Centro Técnico Aeroespacial, Instituto de Aeronáutica e Espaço
CTA/IAE/ASE-N, 12228-904 - São José dos Campos - SP - Brasil
Daniel Strauss
Centro Técnico Aeroespacial, Instituto Tecnológico de Aeronáutica
CTA/ITA/IEAA, 12228-900 - São José dos Campos - SP - Brasil
Luís Fernando Figueira da Silva
Laboratoire de Combustion et de Détonique, UPR 9028 du CNRS
ENSMA et Université de Poitiers, 86960 Futuroscope - France

Abstract. *The work presents a detailed numerical analysis of the order of accuracy of some proposed cell centered, finite volume schemes for the solution of the 2-D gasdynamic equations on triangular unstructured grids. All the schemes analyzed are nominally second order accurate and they are based on a MUSCL-type linear reconstruction of interface properties. The schemes under consideration are also nominally flux-vector splitting-type schemes. The basic aspects effecting the scheme's order of accuracy are the form in which the reconstruction process is implemented and the form in which the limiting process is performed. The schemes are tested on a linear convection-like model equation and the numerical solutions are compared to the analytical solution, for different mesh sizes, in order to assess the scheme's order of accuracy.*

Keywords: *Unstructured grids, Finite volume methods, Flux-vector splitting, 2nd-order reconstruction, Order of accuracy.*

1. INTRODUCTION

Since the pioneering work of Barth and Jespersen (1989), various upwind, nominally second order accurate, finite volume schemes have been proposed in the literature (Durlofsky, Engquist, and Osher, 1992, Lin, Wu, and Chin, 1993, Venkatakrishnan, 1995, Sleigh *et al.*, 1998). In these papers second order accuracy is sough by some kind of gradient evaluation within the control volume, followed by extrapolation of the cell centered properties up to the cell interfaces. Upwinding is achieved via flux vector splitting techniques. Limiting procedures are, then, used in order to guarantee solution monotonicity.

Assessing the effective order of accuracy for unstructured finite volume methods is not a straightforward task, when compared to classical structured finite difference/volume techniques. In these latter cases, an order of accuracy analysis may be performed via Taylor series expansions of the difference scheme. Such an analysis is not applicable when the mesh points connectivity is variable, as is the case for unstructured grid methods. Therefore, numerical computations of model problems seems to be the only avenue to pursue if one seeks to determine the order of accuracy of such methods.

The present work presents a detailed numerical analysis of the order of accuracy of some proposed cell centered, finite volume schemes for the solution of the 2-D gasdynamic equations on triangular unstructured grids (Barth and Jespersen, 1989, Azevedo and Figueira da Silva, 1997). The schemes analyzed are nominally second order accurate, based on a MUSCL-type linear reconstruction of interface properties, and they are also nominally flux-vector splitting-type schemes. The basic aspects effecting the scheme's order of accuracy are the form in which the reconstruction process is implemented and the form in which the limiting process is performed.

Although several different implementations were performed, two basic concepts were tested with regard to the reconstruction process. The first concept essentially attempts to create a one-dimensional stencil normal to the control volume edge of interest and, then, it uses this 1-D stencil in a very straightforward fashion in order to reconstruct interface properties. The other approach is based on computing cell averaged property gradients and using those in order to obtain linear reconstructed interface properties. The schemes are tested on the linear convection-like model equation (Durlofsky, Engquist, and Osher, 1992) and the numerical solutions are compared to the analytical solution, for different mesh sizes, in order to assess the scheme's order of accuracy. The results obtained with the upwind schemes are compared to those computed with the centered Jameson scheme (Jameson and Baker, 1983, and Jameson and Mavriplis, 1986). The results obtained in some cases are, at the same time, interesting and disturbing, indicating that many so-called second order schemes may be quite far from achieving true second-order accuracy, at least in general unstructured triangular grids.

2. PROBLEM FORMULATION

In order to be able to analyze the order of accuracy of unstructured finite volume methods, one needs to numerically solve a model problem. The choice of this model problem is dictated by several constraints. Obviously, the model problem must have a known analytical solution at all times. Another desirable feature is that this solution should be continuous, so that the order of accuracy can be measured by comparison with the computed result via successive refinements of the computational mesh. Moreover, it is essential that the numerical results are not influenced by the conditions arising at the boundaries of the computational domain. With these restrictions in mind, and following the work in Durlofsky, Engquist, and Osher (1992), the authors have chosen as model problem the two-dimensional periodic linear advection problem, using as initial conditions for the scalar quantity a sinus curve in both directions. The computational domain is a square with unity side and the mesh is composed of regular triangles. The analysis starts with a coarse mesh, where the computations are run through one period and the L_1 norm is calculated. The mesh is halved successively, and the computations rerun. The slope of the best fit line, in a least squares sense, through a plot of the logarithm of the L_1 norm as a function of the logarithm of the characteristic size of the mesh gives a measure of the true order of accuracy of the method.

For the scalar, linear model problem considered in the present case, the governing differential equation can be written as

$$\frac{\partial u}{\partial t} + \nabla \cdot \left(\vec{a} u\right) = 0 \quad . \tag{1}$$

Here, u is the dependent variable, $\nabla\cdot(\ )$ is the divergent operator and $\vec{a} = a_x \hat{i} + a_y \hat{j}$ is the constant advection velocity. Moreover, the boundary conditions are periodic on all four sides of the square computational domain.

The governing equations are discretized in a cell centered context in which the discrete vector of conserved variables for the i-th cell is defined as

$$u_i = \frac{1}{V_i} \iint_{V_i} u \, dxdy \quad . \tag{2}$$

The Eq. (1) can, then, be rewritten for each i - th control volume as

$$\frac{\partial}{\partial t}(V_i u_i) + \int_{S_i} (a_x u\, dy - a_y u\, dx) = 0 \quad . \tag{3}$$

It should be observed that, for a cell centered approach, the control volume used for the integration of the governing equations is formed by each triangular cell itself (Batina, 1991). The role of the spatial discretization algorithm is to approximate the surface integral in Eq. (3). This aspect will be discussed in detail in the forthcoming paragraphs.

The present work uses a well-tested, fully explicit, 2nd-order accurate, 5-stage Runge-Kutta time-stepping scheme (Mavriplis, 1988) to advance the governing equations in time.

3. SPATIAL DISCRETIZATION SCHEMES

The primary interest in the present work is to discuss order of accuracy issues associated with the unstructured grid implementation of higher order upwind schemes. In particular, the emphasis is on triangular grids and flux-vector splitting schemes. Hence, a scalar version of Liou's AUSM$^+$ scheme (Liou 1994, 1996) was implemented both as a nominally 1st-order scheme and as a nominally 2nd-order scheme. The 1st-order scheme implementation follows the work of Azevedo and Korzenowski (1998). Moreover, the complete details of the AUSM$^+$ scheme implementation are described in the cited reference, and they will not be repeated here. The basic difference between the scheme in that reference and in the present work is the reinterpretation of the scheme for a linear scalar problem. Therefore, the split interface Mach numbers and convective speeds, as they appear in the original AUSM$^+$ scheme, reduce to the constant advection velocity in the present case. The 2nd-order implementation uses a MUSCL reconstruction (van Leer, 1979). Therefore, the second order scheme follows exactly the same formulation, except that the left and right states that appears in the 1st-order scheme are obtained by a MUSCL extrapolation of the scalar variable. The reconstruction and limiting methods used to obtain the left and right states will be discussed in the forthcoming sections.

For comparison purposes, a centered scheme was also implemented. Again, the current implementation of the centered scheme follows Azevedo and Korzenowski (1998). It is worth noting that, as this scheme is equivalent to a central difference scheme, it is necessary to add artificial dissipation terms to control nonlinear instabilities (Jameson and Mavriplis, 1986).

4. RECONSTRUCTION METHODS

Two basic concepts were tested in the present work with regard to the reconstruction process. The first concept essentially attempts to create a one-dimensional stencil normal to the control volume edge of interest and, then, it uses this 1-D stencil in a very straightforward fashion in order to reconstruct interface properties. The other approach is based on computing cell averaged property gradients and using those in order to obtain linear reconstructed interface properties.

The one-dimensional reconstruction approach is inspired in the work of Lyra (1994). The major difference between the present implementation and the cited reference lies in the direction in which the one-dimensional stencil is constructed. In Lyra (1994), the stencil for extrapolation is constructed along the direction of the edge. Here, since a cell centered finite volume method is of interest, the extrapolation stencil is constructed in a direction normal to the edge.

In an attempt to reinterpret the 1-D ideas in the present unstructured grid context, a line is drawn normal to the edge and passing through the center of the inscribed circle to that triangle. A third point is located over this line, and away from the edge under consideration, at a distance from the center of the inscribed circle equal to the diameter of the circle. The code, then, identifies in which control volume this 3rd point lies, and it uses the properties of this triangle in the linear reconstruction of the primitive variables.

The gradient reconstruction approach followed in the present work consists of attributing cell averaged properties and gradients to the control volume centroid, which allows the linear reconstruction of properties at any point within the cell. Gradients are computed using Green's theorem (Swanson and Radespiel, 1991) and, therefore, transforming derivative calculations into line integrals around appropriate control volumes (in the 2-D case). In the present work the triangles themselves are used as the control volumes for the gradient calculation.

5. LIMITING PROCEDURES

In order to avoid oscillations, extrapolated states must be limited. Several different limiters have been implemented in the present work, including the *minmod*, van Leer, van Albada and *superbee* limiters (Hirsch, 1990). However, the majority of the results discussed here used only the *minmod* limiter. Another aspect concerns the fact that the limiter construction is clearly dependent on the approach used for the linear reconstruction. Hence, the form used to implement the limiter associated with the one-dimensional approach for property reconstruction is different from the one used when the gradient reconstruction is adopted. For the 1-D reconstruction case, the expressions for the limiter, as it was implemented in the present work, can be found in Azevedo and Korzenowski (1998). In the case where gradients are used in the reconstruction, the limiter expressions are similar to that of the previous method. Nevertheless, the ratios of gradients used in the calculation are obtained using the properties at the edge midpoint, which are extrapolated from the centroid properties using the calculated gradients. This is in contrast with the 1-D reconstruction case, which uses the stencil already set up during the one-dimensional property reconstruction for the calculation of the gradient ratios.

6. MESH GENERATION AND BOUNDARY TREATMENT

The model problem considers an extremely simple geometry and, therefore, one would think that triangular mesh generation in this case would be a trivial task. This would indeed be true, except that the authors wanted to have some additional control on the grid being generated and some additional information, beyond the usual unstructured grid information, was necessary in order to truly implement the periodic boundary conditions that the model problem requires. The additional control on the grid was meant to be able to select either a truly unstructured grid or a grid with a user-selected orientation of the triangles. This control would allow the investigation of the grid orientation effect on the order of accuracy of the schemes tested. One should observe that, since the computational domain is a square with unit side length, it is natural to divide the domain into squared control volumes based on the number of subdivisions in each side of the domain. Hence, the triangular grid could be obtained by dividing each quadrilateral volume by one of its diagonals, yielding two triangles. The implementation adopted allows the user to select the division with diagonals oriented with +45° and -45° with respect to the *x* axis.

Therefore, the user can select among three different grids in the present case, namely a truly unstructured grid, in which the orientation of the diagonals is somewhat random, and grids with -45° and +45° for diagonal orientation. The truly unstructured grids were generated using a simplified advancing front method as described by Lo (1985). Examples of the possible grid types are shown in Figure 1.

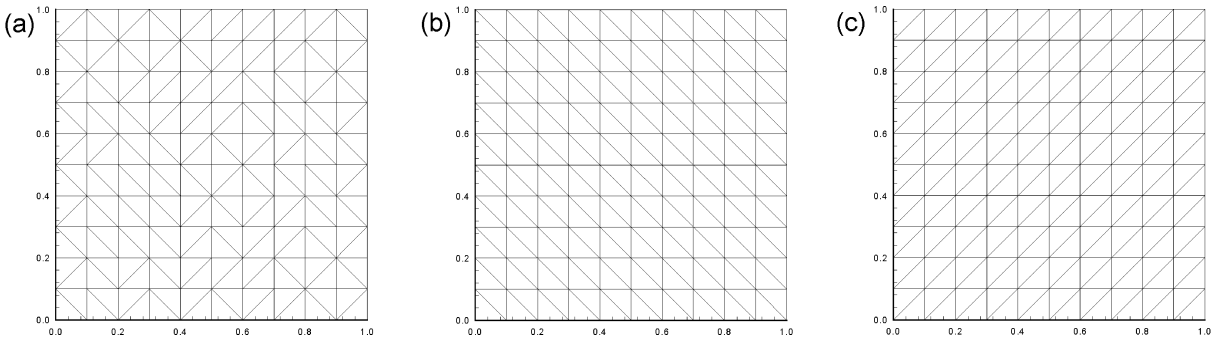

Figure 1: Grid topologies used in the present investigation: (a) truly unstructured grid; (b) diagonals oriented with - 45°; and (c) diagonals oriented with + 45°.

The grids shown in Figure 1 have the coarsest resolution used in the present work, namely with 10 subdivisions along each side of the squared domain or a characteristic length of 0.1. This yields a grid

with 200 triangular control volumes, regardless of the mesh topology adopted. The investigation also considered grids with 20×20, 40×40 and 80×80 divisions. These yield, respectively, a total of 800, 3200 and 12800 control volumes and characteristic lengths of 0.05, 0.025 and 0.0125 dimensionless length units.

The model problem considers periodic boundary conditions along the 4 sides of the squared computational domain. Hence, regardless of the grid topology adopted, the logic in the grid generation routine stores enough information in order to allow an exact implementation of this boundary condition. The procedure stores, for each segment along the boundary, the identification of the corresponding segment along the boundary "on the other side" of the computational domain. Since this is performed in the very early stages of grid generation, the routine has enough information to latter identify corresponding internal triangles along the boundaries which should be used as triangle pairs for periodic boundary condition implementation. Although boundary conditions are implemented through the use of ghost volumes in the present code, the procedure consists in forcing the ghost volume associated with a given triangle along the boundary to receive the property values of the other internal triangle of the pair, previously identified.

7. RESULTS AND DISCUSSION

The work has considered a simple, 2-D, linear, scalar advection problem, as previously described. The main objective of the work is to identify how the error in the solution decreases as the mesh is refined. Hence, all simulations will run the model problem for one period of the solution and, then, compare the numerical solution with the exact solution for the problem. The global error will be measured in terms of the L_1 norm of the difference between exact and numerical results. This can be expressed as

$$L_1 \text{ norm of the error} = \frac{1}{\text{No. Volumes}} \sum_{\text{all volumes}} \left| u_{exact}(x_i, y_i) - u_{num.}(x_i, y_i) \right| \tag{4}$$

where the point with coordinates (x_i,y_i) indicates the centroid of the control volume. One should observe that this is the natural definition of the error for a cell centered finite volume scheme. However, Durlofsky, Engquist, and Osher (1992) point out that one might obtain somewhat different results, in terms of order of accuracy, if some form of averaging of the computational results is performed prior to compute the error.

Hence, a calculation of the L_1 norm of this averaged error was also implemented in the code. In the present case, this averaging was performed by obtaining (averaged) numerical results at the nodes of the control volumes. Therefore, the L_1 norm of this averaged solution at the nodes would be computed using an expression similar to Eq. (4), but with exact and numerical values of u evaluated at the nodal point locations. The averaged numerical values of the function at the nodes are obtained simply by an arithmetic average of the discrete properties of all control volumes which share a given node. This is sufficient for the present case, since all control volumes have the same area. It is possible that, for a more generic mesh, one might have to perform some sort of weighted averaging, using the control volume areas as weights.

The procedure used here to verify the order of accuracy of the proposed schemes consists in running the problem for the four meshes previously defined, with increasing refinement, and plotting the logarithm of the L_1 norm of the error as a function of the logarithm of the mesh spacing. A best fit straight line, in the least square sense, is passed through these points and the line slope determines the order of accuracy of the method.

All tests were run for a constant CFL of 0.1, except for a single test which was run with CFL = 0.01 to make sure the order of time accuracy of the scheme had no effect in the results. Moreover, all upwind solutions used the AUSM$^+$ scheme. Both the cases with linear advection in the x-direction as well as advection along a 45° direction with the x-axis were considered. These two cases correspond, respectively, to the advection velocity $\vec{a} = (a_x,a_y) = (1,0)$ and $(1,1)$. The importance of testing these two cases is associated with an evaluation of the effect of the mesh orientation on the final order of accuracy for the schemes. For some of the triangular grids considered in this investigation, an advection velocity $\vec{a} = (1,1)$ is going to be either aligned with a large number of grid edges or

perpendicular to a large number of grid edges. Hence, it is important to evaluate how this can affect the order of the methods.

The initial tests used the one-dimensional-type of property reconstruction at interfaces for the nominally 2nd-order scheme. The first test case considered a truly unstructured mesh and the convection velocity $\vec{a}$ = (1,0). The results are shown in Figure 2 for the nominally 1st-order scheme and the 2nd-order scheme with the *minmod* and *superbee* limiters. The actual order of accuracy obtained numerically in each case is also presented in Table 1. The L_1 norm of the error for these results was calculated without any averaging procedure, *i.e.*, the error is calculated for properties evaluated at the actual control volume centroid.

Table 1: Order of accuracy for unstructured grid with one-dimensional reconstruction for the case a_x = 1 and a_y = 0.

Method	Order of Accuracy
AUSM$^+$ - 1st order	0.82
AUSM$^+$ - 2nd order with *minmod*	0.94
AUSM$^+$ - 2nd order with *superbee*	0.65

It is clear form the results in Figure 2 and Table 1 that neither nominaly 2nd-order case is even close to true 2nd-order accuracy. Actually, calculations with the *superbee* limiter are yielding an order of accuracy which is smaller than that of the 1st-order scheme. Moreover, the 1st-order scheme is also somewhat worse than true 1st-order, and the 2nd-order scheme with the *minmod* limiter gives a slightly better order of accuracy than the 1st-order scheme. It is also strange that calculations with the *minmod* limiter give better order of accuracy than those with the *superbee* limiter since the former is supposed to be much more dissipative.

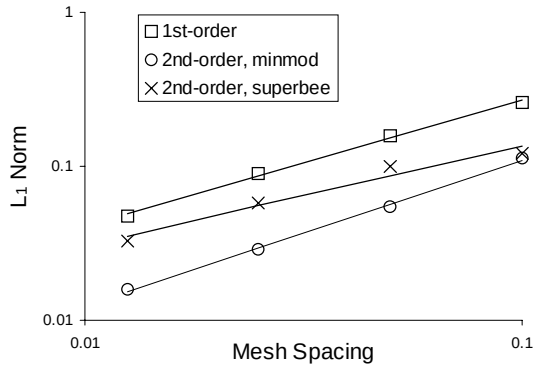

Figure 2: L_1 norm of the error for unstructured grid with one-dimensional reconstruction for the case a_x = 1 and a_y = 0. Lines are least square fits.

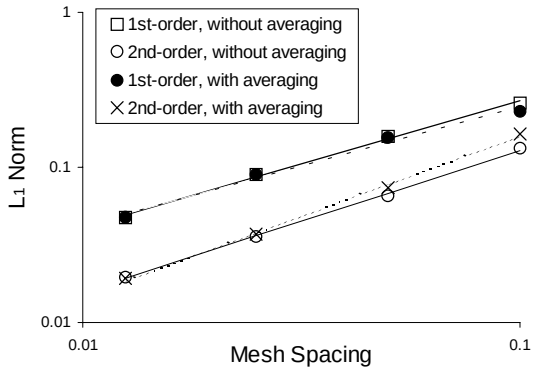

Figure 3: L_1 norm of the error for grid with diagonals oriented -45°, with one-dimensional reconstruction, for the case a_x = 1 and a_y = 0. Lines are least square fits.

Table 2: Order of accuracy for grid with diagonals oriented -45°, with one-dimensional reconstruction, for the case a_x = 1 and a_y = 0.

Method	L_1 Norm without Averaging	L_1 Norm with Averaging
AUSM$^+$ - 1st order	0.82	0.77
AUSM$^+$ - 2nd order	0.91	1.03

A similar analysis for a grid with diagonals oriented -45° with respect to the x-axis, and still considering $\vec{a}$ = (1,0), is presented in Figure 3. The 2nd-order scheme uses the *minmod* limiter. Moreover, both cases in which the error is calculated with and without averaging of numerical property values are presented in this figure. The slope of the least square fits for these cases are indicated in Table 2. One can see that the grid orientation has essentially no effect on the 1st-order

scheme in this case, and it has a small effect on the 2nd-order scheme. Moreover, the solution averaging prior to the error calculation improves the measured order of accuracy for the 2nd-order scheme, which is consistent with the results reported in Durlofsky, Engquist, and Osher (1992). However, it has a small detrimental effect in the measured order of accuracy for the 1st-order scheme. In any event, it is clear from these results that the nominally 2nd-order scheme was quite far from yielding true 2nd-order accuracy.

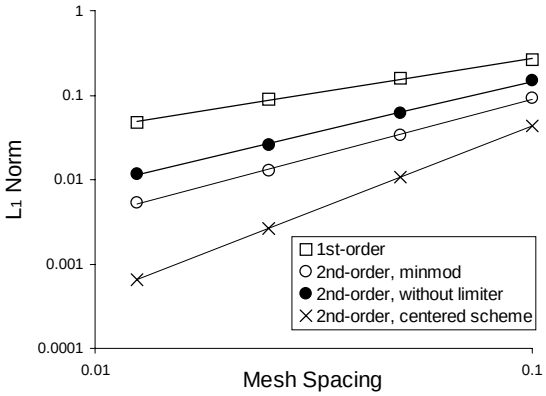

Figure 4: L_1 norm of the error without averaging for grid with diagonals oriented -45°, gradient reconstruction and the case a_x = 1 and a_y = 0. Lines are least square fits.

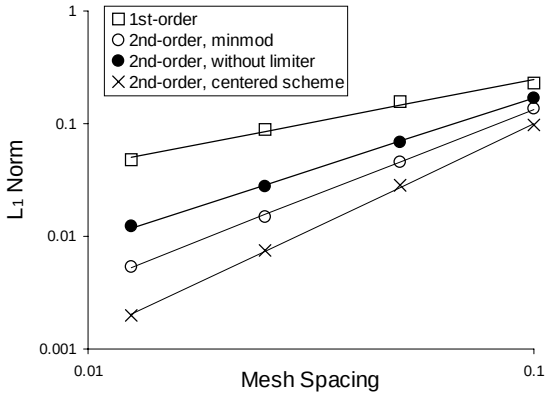

Figure 5: L_1 norm of the error with averaging for grid with diagonals oriented -45°, gradient reconstruction and the case a_x = 1 and a_y = 0. Lines are least square fits.

The next results discussed use property gradient-based reconstruction. The plots for the L_1 norm of the error for a test case with advection velocity given by a_x = 1 and a_y = 0, and using the grid with diagonals oriented with -45°, are presented in Figure 4 for the case in which no averaging of the results is performed before computing the error. The plots for the corresponding cases with averaging of the numerical results prior to the error calculation are shown in Figure 5. These figures show results for the 1st-order upwind scheme and for the 2nd-order upwind scheme with the *minmod* limiter and without any limiter at all. Moreover, for comparison purposes, the figures also show the L_1 norm of the error for the calculations with a 2nd-order centered scheme. The orders of accuracy actually obtained in each case are summarized in Table 3. Clearly, the 1st-order upwind scheme results are the same reported in the previous section, since the form of reconstruction does not affect the 1st-order scheme.

Table 3: Order of accuracy for grid with diagonals oriented -45°, with gradient reconstruction, for the case a_x = 1 and a_y = 0.

Method	L_1 Norm without Averaging	L_1 Norm with Averaging
$AUSM^+$ - 1st order	0.82	0.77
$AUSM^+$ - 2nd order with *minmod*	1.37	1.55
$AUSM^+$ - 2nd order, no limiting	1.23	1.27
2nd order centered scheme	2.01	1.87

The actual order of accuracy obtained with the nominally 2nd-order upwind scheme should be compared, for instance, with the results in Table 2. It is clear from this comparison that the use of gradient reconstruction has yielded better order of accuracy than the 1-D reconstruction process. However, there are some strange features in the results shown in Table 3. For instance, it is not clear why the calculation without any limiter at all yields an actual order of accuracy which is smaller than that obtained when the calculations are performed with the *minmod* limiter. The model problem has a smooth solution, which means that a limiter should actually play no role at all. In the worst case, the limiter might be clipping the smooth peaks and valleys of the smooth model function if it perceives the gradients as too high. But, in any case, there is no reason to obtain better results with the *minmod*

limiter than without any limiter. Furthermore, attempts to run this case with the *superbee* limiter resulted in numerical instability for the finer grids, although a solution could be obtained with the coarsest grid considered.

The calculations summarized in Table 3 also indicate that even the best results obtained with the 2nd-order upwind scheme were still quite far from true 2nd-order accuracy as displayed by the centered scheme. It is also interesting to observe that the averaging of the solution prior to the error calculation consistently improves the numerical order of accuracy of the 2nd-order upwind scheme. However, this is not true for the 1st-order upwind scheme nor for the 2nd-order centered scheme. These results are in contrast with those reported in Durlofsky, Engquist, and Osher (1992), where the averaging always improves the computed order of accuracy. It should be emphasized, however, that the averaging is performed in a different fashion in the present work, when compared to the cited reference. Here, the averaged value of the solution is computed at the nodes of the mesh from the discrete cell-averaged values calculated at the cells by the present cell-centered scheme. In the cited reference, this "averaged value" is computed at the center of the squared cells formed by two adjacent triangles.

A study was also performed to investigate the effect of the CFL number on the present results. For that, a grid with diagonals oriented with +45° was used, together with an advection velocity given by $a_x = 1$ and $a_y = 0$. The AUSM$^+$ scheme with gradient reconstruction and with the *minmod* limiter, was used. The test case was run with CFL = 0.1 and 0.01. The order of accuracy obtained in the various cases analyzed is presented in Table 4. For comparison purposes, the orders of accuracy indicated in Table 4 were calculated using only the results for the three coarsest meshes. This was done because the initial results already indicated that there was no CFL number influence in the order of accuracy of the methods and the cost of running the finest grid with CFL = 0.01 was very high. Moreover, for the cases in which values of the L_1 norm of the error were available for the four grids, *i.e.*, for the cases with CFL = 0.1, the order of accuracy obtained using the results for the four grids is indicated in parentheses in Table 4.

Table 4: Effect of the CFL number on the order of accuracy. Calculations used grid with diagonals oriented +45°, with gradient reconstruction and the *minmod* limiter, for the case $a_x = 1$ and $a_y = 0$.

Method	CFL	L_1 Norm without Averaging	L_1 Norm with Averaging
1st order	0.1	0.77 (0.82)	0.69 (0.77)
1st order	0.01	0.77	0.69
2nd order	0.1	1.42 (1.37)	1.59 (1.55)
2nd order	0.01	1.42	1.59

The effect of grid orientation was investigated by considering grids with a +45° and a -45° orientation for the quadrilateral diagonals used to construct the triangular meshes. The *minmod* limiter was also used in these cases. In order to make any grid effects more evident, the linear advection problem with $a_x = a_y = 1$ was selected for this test case. Moreover, a CFL number of 0.1 was used in the tests. The plots for the L_1 norm of the error are presented in Figure 6 for the case in which no averaging of the results is performed before computing the error. The corresponding results for the cases with averaging of the numerical solution prior to the error calculation are shown in Figure 7. These figures show results for both the 1st-order and 2nd-order schemes. The orders of accuracy actually obtained in each case are summarized in Table 5.

Table 5: Effect of grid orientation on the order of accuracy. Calculations used 2nd-order gradient reconstruction and the *minmod* limiter, for the case $a_x = a_y = 1$.

Method	Grid Orientation	L_1 Norm without Averaging	L_1 Norm with Averaging
1st order	-45°	0.50	0.41
1st order	+45°	0.45	0.45
2nd order	-45°	1.52	1.51
2nd order	+45°	1.49	1.50

Figures 6 and 7, and Table 5 are indicating that, at least for the 2nd-order scheme, this test case shows very little effect of the grid orientation on the scheme's order of accuracy. Moreover, for the advection velocity with $a_x = a_y = 1$, there is also very little difference between the orders of accuracy obtained with and without averaging the solution before the error calculation for the nominally 2nd-order scheme. This situation is in direct contrast with what one sees for the 1st-order scheme. For the 1st-order scheme, there is clearly a mesh orientation effect on the results. One can observe that, for the mesh with +45° orientation, the order of accuracy obtained is independent of averaging and its value is somewhat the average between those obtained with and without averaging for the grid with -45° orientation.

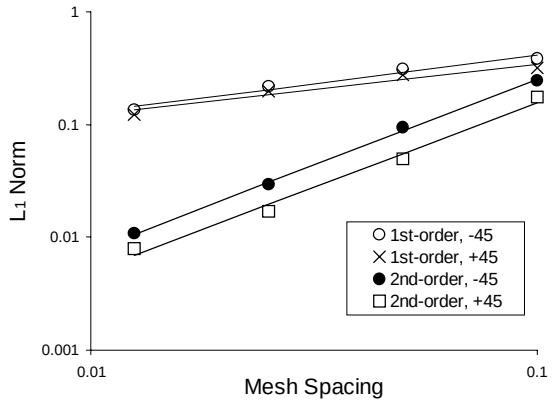

Figure 6: L_1 norm of the error without averaging, gradient reconstruction and *minmod* limiter, for the case $a_x = a_y = 1$. Lines are least square fits.

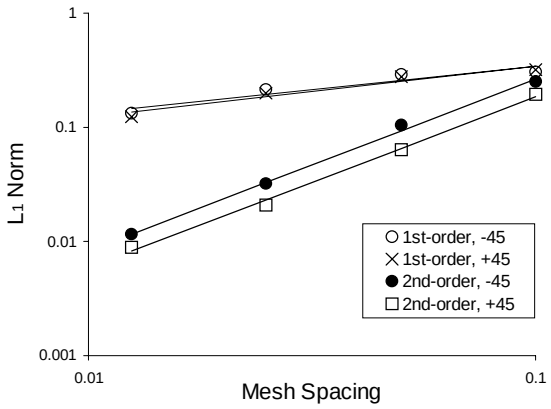

Figure 7: L_1 norm of the error with averaging, gradient reconstruction and *minmod* limiter, for the case $a_x = a_y = 1$. Lines are least square fits.

9. CONCLUSIONS

An assessment of the order of accuracy of some higher order finite volume methods for unstructured grids was performed. The results obtained in some cases are, at the same time, interesting and disturbing. For the one-dimensional reconstruction results some reasoning can be made to explain what caused the poor performance observed. The first idea that comes to mind is the fact that there are reasons to attribute cell averaged values of the properties to the cell centroid. However, the same is not true for attributing cell averaged values to the center of the inscribed circle, which is essentially what the present procedure does. Moreover, the order of accuracy of the scheme could probably be improved if an interpolation is performed in order to obtain the properties at the second points used for the reconstruction. The current implementation simply attributes to these points the cell averaged values of the properties of the triangles within which they are located.

The results with gradient reconstruction yield orders of accuracy quite a lot better than those obtained with the one-dimensional-type reconstruction. Moreover, even though the orders of accuracy achieved for the present cases are still far from true 2nd order, they are much higher than that delivered by the corresponding 1st-order scheme calculations. In particular, for the cases with advection along a 45° direction with the x-axis, the 2nd-order results are about three times better than those with the 1st-order scheme in terms of the actual order of accuracy one can obtain in the numerical calculations. However, as discussed in connection with the results in Table 3, some aspects of the solution behavior with this reconstruction procedure are not fully understood at this point. It is possible that the observed behavior comes from the fact that, when gradients are used, the reconstruction process is truly multidimensional, using information from all neighbors of the triangle under consideration. On the other hand, the limiting procedure does not use information from all neighbors and, hence, it is actually not providing an adequate limiting for the calculation. Therefore, with a gradient-type reconstruction, it is possible that a truly multidimensional limiting procedure is required in order to avoid any problems.

Acknowledgments

This work was accomplished in the framework of an international cooperation agreement between Conselho Nacional de Desenvolvimento Científico e Tecnológico (CNPq) and Centre National de la Recherche Scientifique (CNRS). The authors are indebted to the support of both institutions which has enabled a very fruitful interaction between the research groups represented in the present paper. The authors also gratefully acknowledge the additional partial support of CNPq under the Integrated Project Research Grant No. 522413/96-0.

REFERENCES

Azevedo, J.L.F. and Figueira da Silva, L.F., 1997, The development of an unstructured grid solver for reactive compressible flow applications, AIAA Paper 97-3239, 33rd AIAA/ASME/SAE/ASEE Joint Propulsion Conference & Exhibit, July, Seattle, WA.

Azevedo, J.L.F. and Korzenowski, H., 1998, Comparison of unstructured grid finite volume methods for cold gas hypersonic flow simulations, AIAA Paper No. 98-2629, Proceedings of the 16th AIAA Applied Aerodynamics Conference, June, Albuquerque, New Mexico, pp. 447-463.

Barth, T.J. and Jespersen, D.C., 1989, The design and application of upwind schemes on unstructured meshes, AIAA Paper No. 89-0366, 27th AIAA Aerospace Sciences Meeting, Jan., Reno, NV.

Batina, J.T., 1991, Unstructured-grid methods development – lessons learned. Proceedings of the 4th International Symposium on Computational Fluid Dynamics, vol. I, Sept, Davis, CA, USA, pp. 91-96.

Durlofsky, L.J., Engquist, B. and Osher, S., 1992, Triangle based adaptive stencils for the solution of hyperbolic conservation laws, Journal of Computational Physics, vol. 98, pp. 64-73.

Hirsch, C., 1990, Numerical Computation of Internal and External Flows, Vol. 2: Computational Methods for Inviscid and Viscous Flows, Wiley, New York.

Jameson, A. and Baker, T.J., 1983, Solution of the Euler equations for complex configurations, AIAA Paper 83-1929, July.

Jameson, A. and Mavriplis, D., 1986, Finite volume solution of the two-dimensional Euler equations on a regular triangular mesh, AIAA Journal, vol. 24, n. 4, pp. 611-618.

Lin, S.-Y., Wu, T.-M. and Chin, Y.-S., 1993, Upwind finite-volume method with a triangular mesh for conservation laws, Journal of Computational Physics, vol. 107, pp. 324-337.

Liou, M.-S., 1994, A continuing search for a near-perfect numerical flux scheme. Part I: $AUSM^{+}$, NASA TM-106524, NASA Lewis Research Center, Mar., Cleveland, OH.

Liou, M.-S., 1996, A sequel to AUSM: $AUSM^{+}$, Journal of Computational Physics, vol. 129, n. 2, pp. 364-382.

Lo, S.H., 1985, A new mesh generation scheme for arbitrary planar domains, International Journal for Numerical Methods in Engineering , vol. 21, pp. 1403-1426.

Lyra, P.R.M., 1994, Unstructured grid adaptive algorithms for fluid dynamics and heat conduction, Ph.D. Thesis, Department of Civil Engineering, University of Wales Swansea, Swansea, Wales, U.K.

Mavriplis, D.J., 1988, Multigrid solution of the two-dimensional Euler equations on unstructured triangular meshes, AIAA Journal, vol. 26, n. 7, pp. 824-831.

Sleigh, P.A., Gaskell, P.H., Berzins, M. and Wright, N.G., 1998, An unstructured finite-volume algorithm for predicting flow in rivers and estuaries. Computers & Fluids, vol. 27, n. 4, pp. 479-508.

Swanson, R.C. and Radespiel, R., 1991, Cell centered and cell vertex multigrid schemes for the Navier-Stokes equations, AIAA Journal, vol. 29, n. 5, pp. 697-703.

van Leer, B., 1979, Towards the ultimate conservative difference scheme. V. A second-order sequel to Godunov's method, Journal of Computational Physics, vol. 32, n. 1, pp. 101-136.

Venkatakrishnan, V., 1995, Convergence to steady state solutions of the Euler equations on unstructured grids with limiters, Journal of Computational Physics, vol. 118, pp.120-130.